

Quantum quench dynamics and population inversion in bilayer graphene

Balázs Dóra,^{1,2,*} Eduardo V. Castro,^{3,4} and Roderich Moessner¹

¹Max-Planck-Institut für Physik komplexer Systeme, Nöthnitzer Str. 38, 01187 Dresden, Germany

²Department of Physics, Budapest University of Technology and Economics, Budafoki út 8, 1111 Budapest, Hungary

³Instituto de Ciencia de Materiales de Madrid, CSIC, Cantoblanco, E-28049 Madrid, Spain

⁴Centro de Física do Porto, Rua do Campo Alegre 687, P-4169-007 Porto, Portugal

(Dated: April 22, 2010)

The gap in bilayer graphene (BLG) can directly be controlled by a perpendicular electric field. By tuning the field through zero at a finite rate in neutral BLG, excited states are produced. Due to screening, the resulting dynamics is determined by coupled non-linear Landau-Zener models. The generated defect density agrees with Kibble-Zurek theory in the presence of subleading logarithmic corrections. After the quench, population inversion occurs for wavevectors close to the Dirac point. This could, at least in principle provide a coherent source of infra-red radiation with tunable spectral properties (frequency and broadening). Cold atoms with quadratic band crossing exhibit the same dynamics.

PACS numbers: 81.05.Uw,64.60.Ht,78.67.-n

Charge carriers in bilayer graphene (BLG), which consists of two atomic layers of crystalline carbon, combine non-relativistic "Schrödinger" (quadratic dispersion) and relativistic "Dirac" (chiral symmetry, unusual Berry phase) features. Due to their peculiar nature, BLG holds the tantalising promise of revolutionizing electronics, since its band gap is directly controllable by a perpendicular electric field over a wide range of parameters¹⁻⁵ (up to 250 meV⁶), unlike existing semiconductor technology. Moreover, unlike monolayer graphene (MLG), whose effective model (the Dirac equation) was thoroughly studied in QED and relativistic quantum mechanics, understanding the low energy properties of BLG is a new challenge.

Tuning the gap through zero in BLG in a time dependent perpendicular electric field parallels closely to a finite rate passage through a quantum critical point (QCP): as the gap closes, activated behaviour and a finite correlation length give way to metallic response and power-law correlations, as in a sweep through a QCP. During the latter, defects (excited states, vortices) are produced according to Kibble-Zurek theory^{7,8}. When the relaxation time of the system, which encodes how much time it needs to adjust to new thermodynamic conditions, becomes comparable to the ramping time close to the critical point, the system crosses over from the adiabatic to the diabatic (impulse) regime. In the latter regime, its state is effectively frozen, so that it cannot follow the time-dependence of the instantaneous ground states – as a result, excitations are produced. The theory, general as it is, finds application in very different contexts in physics, ranging from the early universe cosmological evolution⁷ through liquid ^{3,4}He^{8,9} and liquid crystals^{10,11} to ultracold gases¹². The relative ease of manipulating the gap – in particular in real time – via a spatially uniform external electric field, which can therefore play the role of a (time dependent) control parameter, establishes BLG as an ideal setting for the study of quantum quenches with sudden, continuous or any other

sweep protocols¹³⁻¹⁵. This in turn leads to the question: what might such states be useful for?

This complex of questions is addressed here. In particular, we compute the defect (excited state) density after a slow, non-adiabatic passage through a quantum critical point via Kibble-Zurek^{7,8} theory, taking screening between the layers into account. The presence of excited states after such a quench leads to population inversion for wavevectors near the Dirac point in BLG (see Fig. 1), evidenced by the dynamic conductivity. This could in principle provide a coherent source of infra-red radiation with tunable spectral properties (frequency and broadening), determined below in an idealised model. This is tantalising as there are only few materials that generate light in the infrared with tunable frequency, BLG with its unique properties might represent the first step towards new lasers for this regime.

We study the problem in a more general setting of a general class of low energy Hamiltonians, comprising mono- and bilayer graphene, which exhibit quantum critical behaviour, as

$$H = \begin{pmatrix} \Delta & c_J(p_x - ip_y)^J \\ c_J(p_x + ip_y)^J & -\Delta \end{pmatrix}, \quad (1)$$

where J is a positive integer. The energy spectrum is given by $E_{\pm}(p) = \pm\sqrt{\Delta^2 + \varepsilon^2(p)}$ with $\varepsilon(p) = c_J|p|^J$ the gapless spectrum, $|p| = \sqrt{p_x^2 + p_y^2}$ with spatial dimension $d = 2$.

The critical exponents can straightforwardly be read off. The correlation length follows from dimensional analysis: $\xi \sim \hbar(c_J/|\Delta|)^{1/J}$, defining $\nu = 1/J$. The Hamiltonian contains the J th spatial derivative (J th power of p), which leads to $z = J$. The resulting scaling relation $z\nu = 1$ is in agreement with a linearly vanishing gap Δ .

We are interested in the quantum quench dynamics when the gap varies as $\Delta(t) = \Delta_0 t/\tau$ (up to logarithmic corrections, as analyzed below) and $t \in [-\tau, \tau]$. According to Kibble-Zurek scaling^{7,8}, the resulting de-

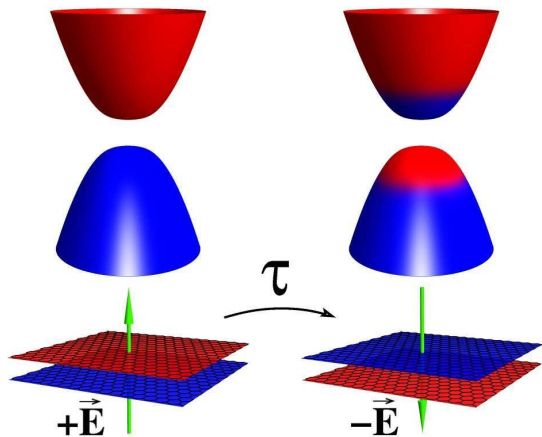


FIG. 1: Reversing the applied perpendicular electric field $+\vec{E}$ in half-filled BLG (left) at a finite rate $1/\tau$ leads to excited states in the upper branch in accordance with the Kibble-Zurek theory of non-equilibrium phase transitions (right). The momentum distribution increases from red (0) to blue (1) in the spectra. Realistic quenching times provide an effective population inversion with little effect on the layer charge asymmetry.

fect (excited state in the upper branch) density is $\rho \sim \tau^{-d\nu/(z\nu+1)}$, which leads to

$$\rho \sim (\Delta_0/\tau)^{1/J}. \quad (2)$$

The matrix structure of Eq. (1) allows us to connect our problem to the Landau-Zener (LZ) dynamics¹⁶ by analysing the solution of

$$i\hbar\partial_t\Psi(t) = H\Psi(t), \quad \Psi(-\tau) = \Psi_-, \quad (3)$$

where $H\Psi_{\pm} = E_{\pm}\Psi_{\pm}$, and the quantity of interest is $\Psi(\tau)$. The exact solution for the diabatic transition probability between final ground and excited states at momentum p for $\varepsilon(p) \ll \Delta_0$ gives for the momentum distribution of excited states in the upper branch (Fig. 1) and and the resulting total defect density

$$P_p = \exp(-\pi\varepsilon^2(p)\tau/\hbar\Delta_0), \quad (4)$$

$$\rho = \frac{A_c}{(2\pi\hbar)^2} \int dp P_p = \frac{A_c\Gamma(1/J)}{4J\pi\hbar^2} \left(\frac{\hbar\Delta_0}{\pi c_J^2\tau}\right)^{1/J} \quad (5)$$

per valley, spin and unit cell, with A_c the unit cell area. This agrees with Kibble-Zurek scaling in Eq. (2). However, the present approach also provides the explicit numerical prefactor for arbitrary J , similarly to the quantum Ising model¹⁷. Note that the bigger J , the larger (and the more insensitive to τ) the resulting defect density, on account of the larger the number of low energy states ($\omega^{2/J}$) within an energy window ω around the Dirac point.

The $J = 1$ case with $c_1 = v_F \approx 10^6$ m/s is realized in MLG¹⁸, where the spinor structure encodes the two sublattices of the honeycomb lattice. The control or even the

very existence of a gap there remains an open issue. Dirac fermions with linear band-crossing can alternatively be realized in optical lattices¹⁹, where the on-site energies of different sublattices are under control, allowing for the introduction of a time dependent mass gap.

The $J = 2$ case with $c_2 = 1/2m$ ($m \approx 0.03m_e$) coincides with the low energy Hamiltonian of BLG²⁰ for energies below $t_{\perp}/4$, with $t_{\perp} \sim 0.3 - 0.4$ eV the interlayer hopping, and the spinor springs from the two layers. Keeping BLG at charge neutrality by either isolating it from the rest of the world in a perpendicular electric field, or by using a dual-gate structure^{3-6,21}, a continuous change of the gate voltage results in closing and reopening the gap, as the density imbalance between the layers is inverted. However, screening due to electron interactions becomes relevant in this case, and the induced gap is related to the external potential, U_{ext} as^{2,22}

$$2\Delta = U_{ext} + \frac{e^2 d \delta n}{2A_c \varepsilon_r \varepsilon_0}, \quad (6)$$

where $\delta n = \sum_p (n_{1p} - n_{2p})$ is the dimensionless density imbalance between the two layers with n_{ip} the particle density of state p on the i th layer. In equilibrium, to a good approximation, the induced gap is given by^{1,2}

$$\Delta = \left(1 + \lambda \ln\left(\frac{4t_{\perp}}{|U_{ext}|}\right)\right)^{-1} \frac{U_{ext}}{2}, \quad (7)$$

and the density imbalance reads

$$\delta n = 4\rho_0 \Delta \ln(|\Delta|/2t_{\perp}), \quad (8)$$

with $\lambda = e^2 d \rho_0 / A_c \varepsilon_r \varepsilon_0 \sim 0.1 - 0.5$ the dimensionless screening strength, $d \approx 3.3$ Å the interlayer distance, ε_0 the permittivity of free space and $\rho_0 = A_c m / 2\pi\hbar^2$ the density of states per valley and spin in the limit $\Delta \rightarrow 0$. For SiO₂/air interface, $\varepsilon_r \approx 2.5$ ($\varepsilon_r = 25$ for NH₃, $\varepsilon_r = 80$ for H₂O), which reduces the effects of screening.

In a quench of a time dependent external potential in BLG, the induced gap couples the two-level systems (stemming from the 2×2 structure of Eq. (1), labeled by p) via the δn term in Eq. (6). The problem would require the solution of a continuum of coupled differential equations, which is not easy, even approximately. We mention that the case of a single level (only one p mode), in which case $\delta n = n_{1p} - n_{2p}$ in Eq. (6), is known as the non-linear LZ model²³, and the resulting dynamics differ qualitatively from the conventional one, possessing nonzero transition probability even in the adiabatic limit for strong non-linear coupling.

The analysis is simplified considerably by the observation that a single level cannot have a strong impact on the dynamics of the others due to the large number of terms in the sum for δn . Thus, it looks natural to replace the non-linear term by an average density imbalance, independent of the explicit time dependence of $n_{1p}(t) - n_{2p}(t)$ for a given p , hence decoupling the LZ Hamiltonians for distinct p 's.

When U_{ext} changes fully adiabatically, the resulting gap and density imbalance are given by Eqs. (7) and (8), respectively. For slow, nearly adiabatic temporal changes of the potential, only a small fraction of terms in the δn sum is expected to behave truly diabatically (contribution from states nearest to the gap edges). Thus we assume that the gap is still given by Eq. (7), and establish self-consistency by verifying that the resulting density imbalance satisfies Eq. (8). Although the usage of Eq. (7) simplifies the picture, it still differs from the conventional LZ form, i.e. subleading logarithmic terms are inevitably present albeit with a reasonably small prefactor λ . Fortunately, one can invoke the extension of the Kibble-Zurek mechanism for non-linear quenches to estimate the resulting defect density^{13,14} (note the difference between a non-linear quench on the LZ problem^{13,14} and the non-linear LZ problem²³). The logarithmic terms in Eq. (7) can be considered as "zerth" powers, therefore the resulting quench is still "linear", with subleading logarithmic corrections.

The inset of Fig. 2 shows the density imbalance, obtained from solving numerically the LZ problem (Eq. (3)) with the adiabatic screening potential (Eq. (7)) for BLG with a linearly varying external potential,

$$U_{ext}(t) = U_0 t / \tau, \quad t \in [-\tau, \tau]. \quad (9)$$

The numerical results are compared to those from Eqs. (7) and (8); the imbalance is rather well described by the equilibrium, fully adiabatic ($\tau \rightarrow \infty$) expression (dashed-green line), therefore our decoupling of the coupled non-linear LZ problem by the adiabatic potential for slow enough quenches with Eq. (7) works satisfactorily. This validates our average field decoupling procedure. Note that to the density imbalance in Eq. (8) all states up to the cutoff, t_\perp , are contributing. On the other hand, defect production occurs at very low energies, close to the touching point of the gapless branches, whose contribution to the imbalance is negligible in the limit of the size of the initial gap, Eq. (7), $\Delta_\lambda \equiv \Delta|_{U_{ext}=U_0} \ll t_\perp$.

The number of defects (excited states in the upper branch) created in an external potential, $U_{ext}(t) = U_0 t / \tau$, $t \in [-\tau, \tau]$, follows Eq. (5) even in the presence of screening as

$$\frac{\rho}{\rho_0 \Delta_0} = \frac{1}{2} \sqrt{\frac{\Delta_\lambda}{\Delta_0}} \sqrt{\frac{\hbar}{\tau \Delta_0}}, \quad (10)$$

where $\Delta_0 = |U_0/2|$, $\Delta_\lambda \equiv \Delta|_{U_{ext}=U_0}$. Eq. (10) together with Eq. (5) are the central results of our Kibble-Zurek analysis. The numerical data fitted with $\rho/\rho_0 \Delta_0 = C(\frac{\hbar}{\tau \Delta_0})^\alpha/2$, and both the prefactor C and the exponent α are compared to the expected values, namely $\sqrt{\Delta_\lambda/\Delta_0}$ for the coefficient and $1/2$ for the τ exponent for various values of λ , summarized in Table I, and shown in Fig. 2. The agreement is indeed remarkable, the slight mismatch in the exponent $1/2$ being due to the subleading logarithmic terms in Eq. (7) for stronger screening. Since $\Delta_0 \rho_0 \sim 10^{-3}$ for $\Delta_0 \sim t_\perp/10$, the resulting density

of defects per unit area (including spin and valley) falls into the order of $\sqrt{\hbar/\tau \Delta_0} \times 10^{12} \text{ cm}^{-2}$, and can take the value $3 \times 10^9 \text{ cm}^{-2}$ for quenching time $\tau \sim 1 \text{ ns}$, corresponding to a ramping rate $\Delta_0/\tau \sim 10^7 \text{ eV/s}$. Note that this density corresponds to the electrons/holes in the otherwise empty/occupied upper/lower branch, and does not by itself imply any particular real space density modulation, since these states contribute negligibly to the layer charge imbalance. A moderately slow quench implies $\tau \Delta_0/\hbar \sim 10 - 100$ with $\Delta_0 \sim t_\perp/10$, translating to $\tau \sim 0.1 - 1 \text{ ps}$. Different non-linear sweep protocols¹³⁻¹⁵ lead to similar conclusion: the steeper (more non-adiabatic) the quench, the bigger the defect density produced.

Our results are robust with respect to variations in the band structure, e.g. extra hopping terms or large asymmetry gap. The quadratic spectrum of BLG with $J = 2$ changes to linear one ($J = 1$) at the vicinity of the Dirac point ($\sim 10 \text{ K}$ range), which could affect the scaling of the defect density ($1/\sqrt{\tau} \rightarrow 1/\tau$) for slow quenches if it was not masked by impurity effects even in the cleanest samples.

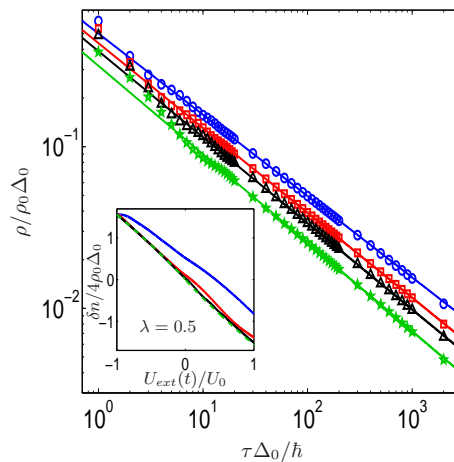


FIG. 2: (Color online) The density of defects created during the quench per spin, valley and unit cell in BLG with screening is shown for $U_{ext} = U_0 t / \tau$, $t_\perp = 5U_0$, $\lambda = 0$ (blue, circle), 0.1 (red, square), 0.2 (black, triangle) and 0.5 (green, star) from top to bottom. The symbols denote the numerical data, the solid lines are fits using $\rho/\rho_0 \Delta_0 = \frac{C}{2} (\frac{\hbar}{\tau \Delta_0})^\alpha$. The inset shows the time dependent density imbalance of BLG per spin and valley in a linear external potential with strong screening ($\lambda = 0.5$) with $\tau \Delta_0/\hbar = 1$ (blue), 10 (red) and 100 (black) from top to bottom. The green dashed line shows the fully adiabatic (equilibrium) result with $\tau \rightarrow \infty$, Eqs. (7)-(8), which is approached fast with increasing τ . Given the simplicity of our self-consistent average field procedure, the agreement is excellent for slow quenches.

Having established the scaling properties of the defect density in BLG, we turn to the determination of the optical response of the excited state resulting from the quench, whose momentum distribution is given by Eq. (4); The occupation number in the upper and lower

λ	0	0.1	0.2	0.5
$\sqrt{\Delta_\lambda/\Delta_0}$ from Eq. (7)	1.00	0.88	0.80	0.64
$\sqrt{\Delta_\lambda/\Delta_0}$ from the fit	1.00	0.87	0.78	0.64
exponent (α)	0.50	0.52	0.53	0.55

TABLE I: The numerically obtained values of the coefficient, $\sqrt{\Delta_\lambda/\Delta_0}$ and the exponent 1/2 of the defect density from Fig. 2 for $t_\perp = 5U_0$, compared to the values based on Kibble-Zurek scaling and Eq. (7).

branches of the spectrum is, respectively, $f_+(p) = P_p$ and $f_-(p) = 1 - P_p$ due to particle-hole symmetry. For momenta close to the K point, population inversion occurs when $f_+(p) > f_-(p)$, i.e. in the energy range $2\Delta_\lambda < \hbar\omega < 2\Delta_\lambda\sqrt{1 + (\hbar\ln 2)/(\pi\Delta_\lambda\tau)}$, which translates in the near adiabatic limit to

$$2\Delta_\lambda < \hbar\omega < 2\Delta_\lambda + \frac{\hbar\ln 2}{\pi\tau}. \quad (11)$$

The effect of a small ac electric field can be considered using Fermi's golden rule, and the initial dynamic conductivity is related to the rate of optical transitions between the two states with the same momentum, weighted by the probabilities of occupied initial and empty final states, as $\Gamma_p(\omega) = \frac{2\pi}{\hbar} M_p^2 \delta(\hbar\omega - 2\sqrt{\Delta_\lambda^2 + \varepsilon^2(p)}) [f_-(p) - f_+(p)]$, where $M_p = |v_x(p)eA|$ is the transition matrix element between the higher and lower energy state, where $v_x(p) = \Psi_+^* \partial H / \partial p_x \Psi_-$ and A the vector potential. Thence, we obtain the dynamic conductivity

$$\sigma(\omega) = \sigma_0 \left[1 - 2 \exp\left(\frac{\pi\tau}{4\hbar\Delta_\lambda} (4\Delta_\lambda^2 - (\hbar\omega)^2)\right) \right] \times \frac{(\hbar\omega)^2 + 4\Delta_\lambda^2}{(\hbar\omega)^2} \Theta(|\hbar\omega| - 2\Delta_\lambda), \quad (12)$$

with $\sigma_0 = e^2/2\hbar$ the ac conductivity of BLG^{24,25}.

Both absorption and stimulated emission are taken into account, and the negativity of the resulting conductivity indicates the dominance of the latter: this indicates a phase coherent response, which is of course essential for a laser. In addition, stimulated emission can

also win against spontaneous emission by increasing the intensity of the incoming radiation field. If spontaneous emission dominates (luminescence), the resulting radiation will still be spectrally limited but without phase coherence.

In the frequency range of Eq. 11, the dynamic conductivity is negative due to the population inversion²⁶ (i.e. the energy injected into the system during the quench is released) as $\sigma(\hbar\omega \rightarrow 2\Delta_\lambda) \approx -2\sigma_0$. The region of negative conductivity shrinks with increasing τ , without influencing the amplitude of $\sigma(\omega)$ precisely at the gap edge. This follows from Eq. (4), implying maximal population inversion at the Dirac point for arbitrary quench time, i.e. $P_{p=0} = 1$.

The typical lasing frequency lies in the close vicinity of Δ_λ (including the THz regime, wavelength of the order of 10 μm), conveniently tunable by perpendicular electric fields⁶. The relaxation times for intra- and interband processes in MLG are estimated as 1 ps and 1-100 ns²⁶, respectively, which might be further enhanced in BLG around half-filling²⁷. Thus, the lasing is expected to survive for quenching times in the ps-ns range even in the presence of the above processes. Repeated quenching (like optical pumping) between Δ and $-\Delta$ is also linked to the Kibble-Zurek theory²⁸ with similar effects on the population inversion.

Our results apply to other systems with a quadratic band crossing, e.g. for certain nodal superconductors or cold atoms on Kagome or checkerboard optical lattices²⁹ at appropriate fillings, described by Eq. (1) with $J = 2$ at low energies. The momentum distribution, Eq. (4) and the concomitant scaling of the defect density after closing and reopening the gap would be direct evidence of the quench dynamics. Particularly intriguingly, graphene multilayers with appropriate stackings realize higher order ($J > 2$) band crossings^{30,31}.

This work was supported by the Hungarian Scientific Research Fund No. K72613 and by the Bolyai program of the Hungarian Academy of Sciences. EVC acknowledges financial support from the Juan de la Cierva Program (MCI, Spain) and the Estímulo à Investigação Program (Fundação Calouste Gulbenkian, Portugal).

* Electronic address: dora@kapica.phy.bme.hu

¹ E. McCann, Phys. Rev. B **74**, 161403(R) (2006).

² E. V. Castro, K. S. Novoselov, S. V. Morozov, N. M. R. Peres, J. M. B. Lopes dos Santos, J. Nilsson, F. Guinea, A. K. Geim, and A. H. Castro Neto, J. Phys.: Condens. Matter **22**, 175503 (2010).

³ J. B. Oostinga, H. B. Heersche, X. Liu, A. F. Morpurgo, and L. M. K. Vandersypen, Nature Mat. **7**, 151 (2007).

⁴ K. F. Mak, C. H. Lui, J. Shan, and T. F. Heinz, Phys. Rev. Lett. **102**, 256405 (2009).

⁵ F. Xia, D. B. Farmer, Y.-M. Lin, and P. Avouris, Nano Lett. **10**, 715 (2010).

⁶ Y. Zhang, T.-T. Tang, C. Girit, Z. Hao, M. C. Martin, A. Zettl, M. F. Crommie, Y. R. Shen, and F. Wang, Nature **459**, 820 (2009).

⁷ T. W. B. Kibble, J. Phys. A **9**, 1387 (1976).

⁸ W. H. Zurek, Nature **317**, 505 (1985).

⁹ C. Bäuerle, Y. M. Bunkov, S. N. Fisher, H. Godfrin, and G. R. Pickett, Nature **382**, 332 (1996).

¹⁰ I. Chuang, R. Durrer, N. Turok, and B. Yurke, Science **251**, 1336 (1991).

¹¹ M. J. Bowick, L. Chandar, E. A. Schiff, and A. M. Srivastava, Science **263**, 943 (1994).

¹² L. E. Sadler, J. M. Higbie, S. R. Leslie, M. Vengalattore,

- and D. M. Stamper-Kurn, *Nature* **443**, 312 (2006).
- ¹³ R. Barankov and A. Polkovnikov, *Phys. Rev. Lett.* **101**, 076801 (2008).
- ¹⁴ D. Sen, K. Sengupta, and S. Mondal, *Phys. Rev. Lett.* **101**, 016806 (2008).
- ¹⁵ C. De Grandi, V. Gritsev, and A. Polkovnikov, *Phys. Rev. B* **81**, 012303 (2010).
- ¹⁶ N. V. Vitanov and B. M. Garraway, *Phys. Rev. A* **53**, 4288 (1996).
- ¹⁷ J. Dziarmaga, *Phys. Rev. Lett.* **95**, 245701 (2005).
- ¹⁸ A. H. Castro Neto, F. Guinea, N. M. R. Peres, K. S. Novoselov, and A. K. Geim, *Rev. Mod. Phys.* **81**, 109 (2009).
- ¹⁹ A. Dutta, R. R. P. Singh, and U. Divakaran, *EPL* **89**, 67001 (2010).
- ²⁰ E. McCann and V. I. Fal'ko, *Phys. Rev. Lett.* **96**, 086805 (2006).
- ²¹ S. Kim and E. Tutuc, *Quantum Hall effect in dual-gated graphene bilayers with tunable layer density imbalance*, arXiv:0909.2288.
- ²² H. Min, B. Sahu, S. K. Banerjee, and A. H. MacDonald, *Phys. Rev. B* **75**, 155115 (2007).
- ²³ B. Wu and Q. Niu, *Phys. Rev. A* **61**, 023402 (2000).
- ²⁴ D. S. L. Abergel and V. Fal'ko, *Phys. Rev. B* **75**, 155430 (2007).
- ²⁵ E. J. Nicol and J. P. Carbotte, *Phys. Rev. B* **77**, 155409 (2008).
- ²⁶ V. Ryzhii, M. Ryzhii, and T. Otsuji, *J. Appl. Phys.* **101**, 083114 (2007).
- ²⁷ M. Monteverde, C. Ojeda-Aristizabal, R. Weil, M. Ferrer, S. Gueron, H. Bouchiat, J. N. Fuchs, and D. Maslov, arXiv:0903.3285.
- ²⁸ V. Mukherjee, A. Dutta, and D. Sen, *Phys. Rev. B* **77**, 214427 (2008).
- ²⁹ K. Sun, H. Yao, E. Fradkin, and S. A. Kivelson, *Phys. Rev. Lett.* **103**, 046811 (2009).
- ³⁰ F. Guinea, A. H. Castro Neto, and N. M. R. Peres, *Phys. Rev. B* **73**, 245426 (2006).
- ³¹ H. Min and A. MacDonald, *Phys. Rev. B* **77**, 155416 (2008).